

The Shape of Dark Matter Halos

Penny D. Sackett

Kapteyn Astronomical Institute, 9700 AV Groningen, The Netherlands

Abstract.

Techniques for inferring the radial and geometric form of dark matter halos and the results they have produced to date are reviewed. Dark halos appear to extend to at least ~ 50 kpc with total enclosed masses that rise linearly with radius R . Whether this behavior can be extrapolated to distances as large as 200 kpc and beyond is controversial; results at this radius are model-dependent. Observationally, the geometrical form of the dark halo can be characterized by the equatorial axis ratio $(b/a)_\rho$ (ovalness) and vertical-to-equatorial axis ratio $(c/a)_\rho$ (flattening) of the total density. Different techniques consistently yield $(b/a)_\rho > 0.7$ (and thus $(b/a)_\Phi > 0.9$) at $R \sim 20$ kpc, with more axisymmetric values, $(b/a)_\rho \gtrsim 0.8$, being more likely. Results are less consistent for the vertical flattening, perhaps due to the difference in the spatial regions probed by different techniques or inappropriate assumptions. Techniques that probe furthest from the stellar plane ($z \sim 15$ kpc) consistently implicate substantially flattened $(c/a)_\rho = 0.5 \pm 0.2$ dark halos. These axis ratios are in acceptable agreement with expectations from N-body simulations of cold dark matter mixed with $\sim 10\%$ dissipational gas.

1. Introduction

A large portion of galactic dynamics is the study of the relationship between mass and motion in and around galaxies. The total gravitational potential of galaxies — its extent, radial density profile, flattening, and triaxiality — strongly affects the motions and morphology of associated stellar and gaseous components, and thus subjects as varied as merging rates, the evolution of galactic disks, bars, warps and spiral structure, the Tully-Fisher and Fundamental Plane relations, and the nature of the presumed galactic dark matter constituents.

To the extent that the strength of the gravitational potential of galaxies is provided by unseen dark matter — rather than by poorly characterized luminous mass or a modification to the Law of Gravitation (McGaugh 1999, and references therein) — the morphology and motion of luminous galactic tracers can be used to deduce the form of the underlying dark mass distribution, provided that the relationship linking them is sufficiently well understood. Each luminous tracer has its own advantages and disadvantages for this purpose; many are suitable only for galaxies of a given type or within a given galactocentric radius.

Several observational techniques and the results that they have produced regarding dark halo shape are reviewed here, with emphasis on the strengths

and weakness of each. Many of the results are model-dependent; some are in apparent conflict with others. In this brief and necessarily incomplete review, it will not be possible to do justice to the complexity and richness of the scientific dialogue on these issues or to resolve apparent discrepancies. Instead, emphasis will be placed on the assumptions and possible systematic effects inherent to various techniques, and on the areas of general agreement and controversy between them. The focus will be on spirals rather than early type galaxies, in part because the shape of dark halos is (generally) better constrained in disk galaxies but also because the situation with respect to ellipticals is reviewed elsewhere in this proceedings (Bridges 1999). For other reviews on the shape of dark halos, see Rix (1996) and Sackett (1996).

2. What do we mean by halo shape?

The shape of the dark halo is determined by its radial profile and — to the extent that it can be described as triaxial — the axis ratios b/a (intermediate-to-long) and c/a (short-to-long). As we shall see, most all observational studies indicate that, in the region where they can be probed, dark halos are only mildly triaxial and oblate ($b \approx a$), with the equatorial plane of the dark halo nearly coinciding with that of the stellar body. Throughout this review, we will characterize the geometric form of the dark halo by $(b/a)_\rho$ and $(c/a)_\rho$, the axis ratios of *density*, not potential. The gravitational potential Φ to which any density ρ gives rise will in general be more spherical; a rough rule of thumb is

$$1 - (c/a)_\rho \equiv \epsilon_\rho \approx 3 \epsilon_\Phi \equiv 3 [1 - (c/a)_\Phi] \quad . \quad (1)$$

To first approximation, closed loop orbits of a tracer population will have the same ellipticity as the underlying potential, but their long axis will be perpendicular to that of Φ .

In the most general case, $(b/a)_\rho$ and $(c/a)_\rho$, which describe the ovalness and flattening of the dark density respectively, may be functions of radius. At a given radius, the shape of the total gravitational potential may differ from that due to the dark halo alone, depending on the relative shape and strength of the luminous and dark contributions to the total Φ at that position.

3. Radial Profile of the Dark Halo

The mass of the halo within a given enclosed radius depends strongly on the form of its radial density profile $\rho(r)$. The inner radial profile of the dark halo affects the dynamic interplay between dark matter and mature stellar systems, while the outer profile influences the dynamics of the galaxy-satellite system and its interaction with its nearest neighbors.

3.1. How much dark mass is in the central regions of galaxies?

The quality of galactic rotation curves allows the accurate determination of the total (luminous + dark) mass enclosed within a radius equal to one-half the maximum extent R_{TRACER} of the velocity tracer (Sackett 1997). If the isodensity contours of total mass are not concentric ellipsoids, as they are unlikely

to be when composed of several components of differing shape, uncertainties in the extrapolation of the outer rotation curve translate into uncertainties in the inferred enclosed mass beyond R_{TRACER} . Interior to R_{TRACER} , uncertainty in the *dark* density profile $\rho(r)$ is not due to uncertainty in dark halo geometry or inadequate velocity data, but to the uncertain mass-to-light ratio M/L of the luminous component and thus the contribution of the luminous mass to the inner rotation support of the galaxy.

The “maximum disk hypothesis,” which assumes that the mass of the stellar disk alone (possibly in conjunction with a stellar bulge) is responsible for the inner rotation speed of spirals, was first formulated in order to place a conservative lower limit on the amount of dark matter deduced from rotation curves (van Albada & Sancisi 1986). Since then, evidence both for and against the suitability of the hypothesis as a description of the actual distribution of stellar mass in the interiors of bright, high surface-brightness spirals has been put forward (e.g., Palunas & Williams 1999; Courteau & Rix 1999, Sellwood 1999, and references therein). Mounting evidence suggests that dwarfs and low surface brightness spirals are dominated by dark matter at all radii (de Blok & McGaugh 1997), though this conclusion may not be universal (Swaters 1999).

3.2. How far do dark halos extend?

In spirals, the neutral hydrogen gas layer has an outer radius of 30 kpc; planetary nebulae and globular clusters can be used to probe similar radii in ellipticals (Bridges 1999). These tracers are generally consistent with an isothermal *total* mass distribution ($M(< R) \propto R$). In order to probe the outer radial profile and total extent of dark matter halos, a visible tracer at larger radii is required (Table 1).

Model potentials of the Milky Way built to support the orbits inferred from radial velocities and proper motions of the Magellanic Clouds and Stream yield a total of the Milky Way of $(5.5 \pm 1) \times 10^{11} M_{\odot}$ inside 100 kpc (Lin, Jones & Kremola 1995), about half of which must lie outside the present Cloud distance (~ 50 kpc). To reconcile this with larger estimate of $(5.4 \pm 1.3) \times 10^{11} M_{\odot}$ inside 50 kpc necessitated by the enforcement of Local Group timing constraints and inclusion of Leo I as a satellite (Kochanek 1996), requires that the Galaxy have a dark mass of $\sim 2.5 \times 10^{11} M_{\odot}$ and a total of mass of $\sim 3.0 - 3.5 \times 10^{11} M_{\odot}$ interior to 50 kpc (Sackett 1996). Such a mass distribution would have a lower circular velocity — as advocated by many authors, most recently Merrifield & Olling (1998) — than the current IAU standard value of 220 km s^{-1} .

The dark distribution of the Galaxy is thus likely to extend to at least 100 kpc. Satellite kinematics have been used to argue that the mass distribution of both the Milky Way (Zaritsky 1998) and external galaxies (Zaritsky & White 1994) extends isothermally to more than 200 kpc, though this conclusion is in conflict with that of an earlier, smaller study that combined information from rotation curves and satellites to conclude that galactic potentials were already keplerian at 3 disk radii (Erickson, Gottesman & Hunter 1987).

Satellites at the largest distances (200-300 kpc) from their primaries, where they are sure to probe the dark potential, have orbital times are on the order of a Hubble time; their non-equilibrium kinematics and distribution can only be studied in the context of a halo formation model. The advantage of a cold,

Table 1. Inferred Extent of Dark Halos^a

Method/Tracer Reference	System	Extent (kpc)	Inferred Quantities	
			Mass ($10^{11} M_{\odot}$)	M/L^b (M_{\odot}/L_{\odot})
Magellanic Cloud and Stream Orbits Lin, Jones & Kremola 1995	Milky Way	$\gtrsim 100$	2.8 (< 50 kpc) 5.5 (<100 kpc)	— —
Satellite Kinematics Kochanek 1995	Milky Way	$\gtrsim 100$	5.4 (< 50 kpc) 8.0 (<100 kpc)	— —
Erickson, Gottesman & Hunter 1987	Nearby spirals	$\lesssim 100$	—	20
Zaritsky & White 1994	Distant spirals	$\gtrsim 200$	~ 20 (<200 kpc)	110 – 340
Giant Ring Kinematics Schneider 1995	Leo HI Ring	$\lesssim 60$	5.6 (<100 kpc)	25
Tidal Tail Length Dubinski, Hernquist & Mihos 1996	Simulations	$\lesssim 100$	—	—
Statistical Weak Lensing Brainerd, Blandford & Smail 1996	Lum-Selected	> 30	13_{-7}^{+16} (<130 kpc)	—

^a $H_0 = 75 \text{ km s}^{-1} \text{ Mpc}^{-1}$ used throughout.

^bMass-to-Light ratio within maximum extent.

smooth tracer like HI gas over a hot discrete collection of satellites is that the orbit structure can be traced on the sky adding to the information gained from radial velocities. The HI ring in Leo completely encircles the early-type galaxies M105 and NGC 3384 at a radius of 100 kpc. The radial velocities and spatial distribution of the gas are consistent with a single, elliptical *keplerian* orbit with a center-of-mass velocity equal to the centroid of the galaxy pair, and a focus that can be placed at the barycenter of the system without compromising the fit (Schneider 1995), suggesting that the dark matter in this system does not extend much beyond the ring pericenter radius of 60 kpc.

The presence of long (50 – 100 kpc) tidal tails seen in HI emission in many interacting systems has been used to argue that dark halos must be more compact and/or less massive than those predicted by standard ($\Omega = 1$) cold dark matter cosmologies or inferred from the basis of satellite studies (Dubinski, Mihos & Hernquist 1996; Mihos, Dubinski & Hernquist 1998). In particular, it was claimed that the dark halo could contribute no more than $\sim 90\%$ of the total enclosed mass. This has been challenged by Springel & White (1998) who argue that if the size and angular momentum of the disk and halo are linked, massive halos may generate long tidal tails because the disks are larger as well. Dubinski, Mihos & Hernquist (1999) agree with this conclusion, but conclude that the falling rotation curves then required at the edges of disks to produce long tidal tails may be at odds with large isothermal halos inferred by other methods.

The tangential distortion of background galaxies due to weak lensing by foreground galaxies is statistically measurable for large samples of source-lens pairs and high quality data. Brainerd, Blandford & Smail (1996) obtain a mass of $13_{-7}^{+16} \times 10^{12} M_{\odot}$ within 130 kpc with this method, although the 1σ uncertainty on the truncation radius allows halo extents as small as 30 kpc.

4. Non-axisymmetry of Dark Halos: $(b/a)_\rho$

Are spiral galaxies axisymmetric ($b = a$) or are the equidensity contours oval in the stellar equatorial plane? Table 2 lists observational attempts to answer this question, where $(b/a)_\rho$ is the inferred axis ratio of the isodensity contours at the indicated radius.

Assuming that intrinsic ovalness of the stellar disk can be used to trace the non-axisymmetry of the underlying density, the statistical distribution of observed axis ratios on the sky can be related to $(b/a)_\rho$: the more elongated the density, the fewer galaxies will be observed with $(b/a)_{\text{LUM}} \approx 1$. Recent attempts to use this method (e.g., Lambas, Maddox & Loveday 1992; Fasano et al. 1993) with the APM and RC3 surveys find that while the stellar bodies of ellipticals and early type spirals appear to have some degree of triaxiality, spirals are more axisymmetric. A mean deprojected axis ratio of $(b/a)_{\text{LUM}} = 0.9$ was found for isophototal contours of the APM spirals, and a sample of unbarred RC3 spirals yielded $(b/a)_{\text{LUM}} = 0.93$. Assuming that the stellar distribution traces the potential of the underlying mass distribution (Eq. 1), and mindful of the complications of bar and spiral structure, the lower limit on the axis ratio of dark isodensity contours in the plane can be taken as $(b/a)_\rho \gtrsim 0.7 - 0.8$.

If perfectly face-on systems could be found and their axis ratios measured in a wavelength that is free of contamination from dust and the spiral structure caused by bright young populations, a more reliable estimation of the axisymmetry the potential might be obtained. Rix & Zaritsky (1995) attempted this using K band imaging and small HI linewidths as a selection for face-on systems. The result indicates a small but persistent non-axisymmetry of $(b/a)_\Phi = 0.955$ in the potential corresponding to $(b/a)_\rho \approx 0.85$ for the underlying density distribution.

Table 2. Observational Constraints on Dark Halo Non-axisymmetry^a

Method/Tracer Reference	System	R Extent Probed (kpc)	$(b/a)_\rho$
Sky distribution of axis ratios			
Lambas, Maddox & Loveday 1992	APM Survey Spirals	Opt Radius	$\gtrsim 0.7$
Fasano et al. 1993	Unbarred RC3 Spirals	Opt Radius	$\gtrsim 0.8$
K Band Imaging			
Rix & Zaritsky 1995	Small HI Linewidths	K Band Radius	0.77-0.93
Gas and Star Kinematics			
Kuijken & Tremaine 1994	Milky Way	8 - 16 kpc	0.75
HI Ring Kinematics			
Franx, van Gorkom & de Zeeuw 1994	E/S0 IC 2006	~ 13 kpc	0.96 ± 0.08
Harmonic Analysis of Gas Kinematics			
Schoenmakers 1998, 1999	HI-rich Spirals	1 - 2 Opt Radii	0.85 ± 0.04
Low Scatter in Tully-Fisher Relation			
Franx & de Zeeuw 1992	Spirals	HI Gas Radius	$\gtrsim 0.84$

^aFor some references, $(b/a)_\rho$ has been estimated from ϵ_Φ using Eq. 1.

The neutral hydrogen layer in spirals extends to comparable or larger radius than the light and thus might be expected to be a better probe of the axisymmetry of the dark halo. At these radii, the gas is further from the disturbances in the potential caused by bars and stellar spiral structure (though spiral structure is often seen in the HI gas itself). The cold dynamical state of HI and its

dissipational nature makes it more likely to follow the closed loop orbits that are a good indication of isopotential contours in the disk plane.

Kuijken & Tremaine (1994) have suggested that part of the apparent discrepancy between the rotation curves constructed from stellar and gaseous tracers in the Milky Way may be due to the fact that they are located at different positions within an inherently non-axisymmetric potential. Their attempts to resolve these discrepancies requires that the line-of-sight to the Sun lie near the short axis of the potential and leads to an estimate of $\epsilon_\Phi = 0.08$ for the equipotential ellipticity at $1 - 2 R_0$ (8-16 kpc), corresponding to $(b/a)_\rho = 0.75$.

Assuming that the HI gas ring in the E/S0 IC 2006 lies in the galaxy's symmetry plane, its shape and kinematics indicate that the isodensity contours of the total mass distribution at ~ 13 kpc (assuming pure Hubble flow at $75 \text{ km s}^{-1} \text{ Mpc}^{-1}$) are consistent with perfect axisymmetry, with $(b/a)_\rho = 0.96 \pm 0.08$ (Franx, van Gorkom & de Zeeuw 1994). The technique applied to the ring IC 2006 can be extended to the filled gas disks typical of spirals (Schoenmakers, Franx & de Zeeuw 1997) and used to study two-dimensional HI velocity fields measured via 21cm synthesis mapping. The measured value depends on the (unknown) viewing angle with respect to the short axis of the potential; averaging over random viewing angles yields a mean value of $(b/a)_\rho = 0.85 \pm 0.04$ for a sample of 7 field spirals (Schoenmakers 1998, 1999).

All of this evidence is consistent with $(b/a)_\rho \gtrsim 0.7$ at the edge of the optical disk or just beyond. Random viewing angles would cause the gas in oval orbits to be viewed at different positions, inducing scatter in the measured HI linewidth at a given absolute magnitude; the small scatter in the Tully-Fisher relation limits this ovalness in the total density to $(b/a)_\rho > 0.7$ (Franx & de Zeeuw 1994). Given that there are other sources for scatter in the Tully-Fisher relation, the true constraint may lie closer to $(b/a)_\rho > 0.84$. Similarly, given other possible sources of non-axisymmetry, such as warping, possible non-equilibrium gas orbits (due to recent accretion), and bar and spiral structure, most values in Table 2 should be considered lower limits to the axis ratio of the dark density distribution, which is more likely to be $(b/a)_\rho \gtrsim 0.8$ near the outskirts of spirals.

5. Flattening of Dark Halos: $(c/a)_\rho$

The question of whether dark matter is distributed in a spherical $(c/a)_\rho = 1$ halo, a flattened halo, or a disk-like $(c/a)_\rho \lesssim 0.2$ structure is important not only because of the implications for galactic dynamics, but also because of the suggestion that galactic dark may be baryonic and dissipative, e.g., clumps of cold gas in the disk (Pfenniger, Combes & Martinet 1994). The question cannot be answered by traditional rotation curve analysis; luminous tracers capable of probing of the vertical gradient of the gravitational potential are required. In Table 3 several such tracers that have been used for this purpose are listed together with the vertical-to-equatorial axis ratio $(c/a)_\rho$ inferred from their study.

The anisotropy in the velocity dispersion of Population II halo stars has been used by several authors to estimate the flattening of the Milky Way mass distribution near the solar radius (Binney, May & Ostriker 1987, van der Marel 1991, Amendt & Cuddeford 1994). Due to uncertainties in Galactic parameters and particularly the orbital structure of the tracer stars, these studies have

remained largely inconclusive, with results in the range $0.3 < (c/a)_\rho < 1$. Modeling the velocity distribution of local stars with Hipparcos proper motions has resulted in the constraint that the local scale height of the total mass must be larger than ~ 2 kpc, while the density scale length is estimated to be 1.8 ± 0.2 kpc (Bienaymé 1999). These measurements are complicated by indications that the flattening of the tracer population and the shape of its orbit structure may change with radius (e.g., Sommer-Larsen et al. 1997, and references therein.)

Table 3. Observational Constraints on Dark Halo Flattening

Method/Tracer Reference	System	z Extent Probed (kpc)	$(c/a)_\rho$
Population II Kinematics			
Binney, May & Ostriker 1987	Milky Way	~ 20 kpc	$0.3 - 0.6$
van der Marel 1991	Milky Way	~ 20 kpc	> 0.34
Amendt & Cuddeford 1994	Milky Way	< 50 kpc	~ 0.7
3-D Kinematics of Local Disk Stars			
Bienaymé, O. 1999	Milky Way	—	$(z_0)_\rho > 2$ kpc ^a
Geometry of X-ray Isophotes			
Buote & Canizares 1996	S0 NGC 1332	~ 15 kpc	$0.28 - 0.53$
Buote & Canizares 1997	E4 NGC 720	~ 10 kpc	$0.37 - 0.60$
Buote & Canizares 1998	E4 NGC 3923	~ 13 kpc	$0.34 - 0.65$
Kinematics of Polar Rings			
Arnaboldi et al. 1993	E4 AM2020-504	~ 5 kpc	~ 0.6
Sackett et al. 1994	E7 NGC 4650A	~ 17 kpc	$0.3 - 0.4$
Sackett & Pogge 1995	E4/5 A0136-0801	~ 12 kpc	~ 0.5
Combes & Arnaboldi 1996	E7 NGC 4650A	~ 17 kpc	> 0.2
Precession of accreted dusty gas disk			
Steiman-Cameron, Kormendy & Dusisen	SO NGC 4753	few kpc	$0.84 - 1.0$
Evolution of Gaseous Warps			
Hofner & Sparke 1994	5 Spirals	few kpc	$0.6 - 0.9$
New et al. 1998	5 Spirals	few kpc	> 0.85
Flaring of HI Gas Layer of Spirals			
Olling 1996	Sc NGC 4244	few kpc	$0.1 - 0.5$
Olling & Merrifield 1997	Milky Way	few kpc	$0.5 - 1.0$
Becquaert & Combes 1997	NGC 891	few kpc	$0.2 - 0.5$
Strong Radio Lensing of Spirals			
Koopmans, de Bruyn & Jackson 1998	B1600+434	—	> 0.4

^aHere $(z_0)_\rho$ is the disk scale height of the total density.

Buote & Canizares (1996, 1997, 1998) have measured the flattening of extended X-ray isophotes which, if the gas is in hydrostatic equilibrium, should trace the shape of the underlying potential in the early-type hosts. Their results, which are independent of assumptions about X-ray gas temperature, indicate substantially flattened dark mass axis ratios of $0.28 < (c/a)_\rho < 0.65$, equal to or more flattened than the optical light in each system. Isophote twists in NGC 720 indicate a possible misalignment of the luminous and dark components.

Accreted gas appears to settle onto orbits that are near the equatorial or polar planes of galaxies, suggesting that the underlying potential is not spherical. The shape and kinematics of polar rings are excellent probes of $(c/a)_\rho$; these rare rings of gas and stars can extend to 20 stellar disk scale lengths in orbits nearly perpendicular to the equatorial stellar plane. Pioneering work on the kinematics of polar rings yielded slightly flattened halos with very large uncertainties (Schweizer, Whitmore & Rubin 1983, Whitmore, McElroy & Schweizer

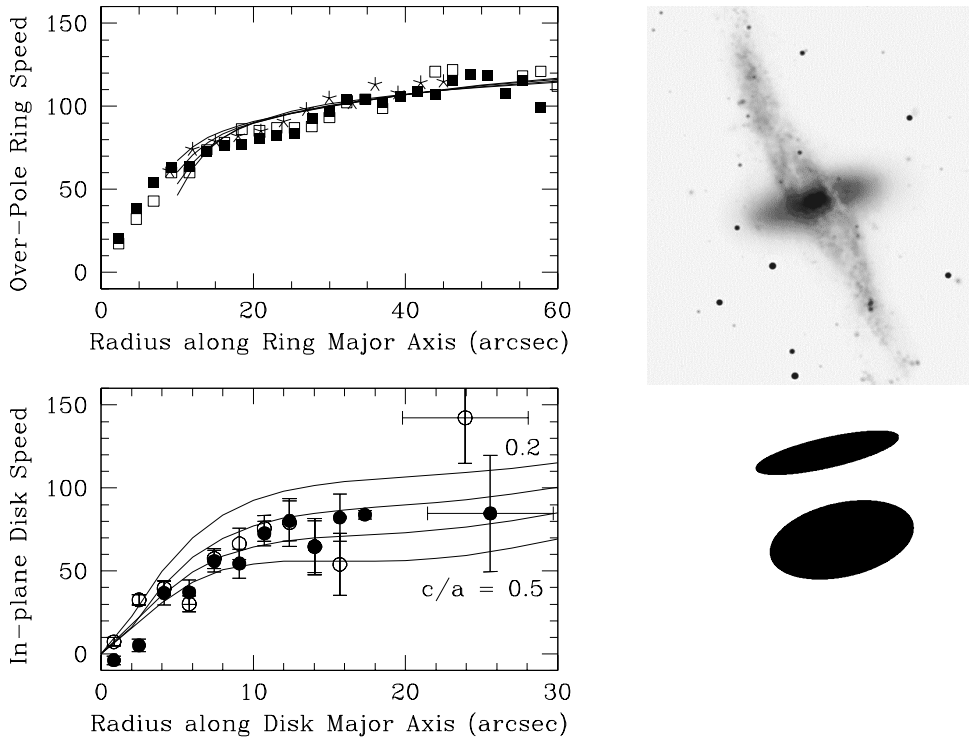


Figure 1. *Left:* Mass models for polar ring galaxy NGC 4650A with different dark halo flattening are adjusted to fit the ring kinematics (top). Only those with $0.3 < c/a < 0.4$ are able to match disk star kinematics of the main galaxy (bottom). *Top Right:* NGC 4650A as seen in one of the first images of the VLT at the European Southern Observatory. *Bottom Right:* Morphology of dark halo shapes considered in left panel; the best-fitting halo shape is intermediate to those shown. (Adapted from Sackett et al. 1994).

1987). Subsequent studies using more detailed mass models and higher quality data over a larger radial range narrowed the range of dark density flattenings to $0.3 \lesssim (c/a)_\rho \lesssim 0.6$ (Arnaboldi et al. 1993, Sackett et al. 1994, Sackett & Pogge 1995). In each case, the inferred dark halo flattening is aligned with and comparable to that of the stellar body, as illustrated for NGC 4650A in Fig. 1.

Combes & Arnaboldi (1996) have also suggested that the dark matter distribution of NGC 4650A may be highly flattened, but toward the plane of the ring itself and thus misaligned from the flattened stellar body by 90° . Their ring model requires a stellar mass-to-light ratio of $M/L_B = 5$ and a constant inclination angle of 85° (to produce a large line-of-sight correction to the ring velocities), that appear to be inconsistent with the color of the ring and its inclination as derived from optical imaging and $H\alpha$ velocity fields.

The substantially flattened halos inferred from X-ray gas and polar ring studies contrast sharply with those inferred from the kinematics of gas disks close to the equatorial plane. In order to fit the complicated pattern of dust lanes in the SO NGC 4753, a precessing disk model was used by Steiman-Cameron,

Kormendy & Durisen (1992). The flattening is coupled to the assumed viscosity and age of the structure: if it has completed 6 or more orbits at all radii, the flattening must be quite modest, $(c/a)_\rho \geq 0.84$ to avoid excessive winding.

New et al. (1998) have applied a similar precessing, viscous, disk model in scale-free potentials to fit the warps observed in five spirals. They find that η_Φ , a measure of the strength of the quadrupole moment, must be small ($10^{-3} < \eta_\Phi < 10^{-2}$), implying density axis ratios of $0.85 < (c/a)_\rho \lesssim 1$ for nearly axisymmetric structures older than one-tenth a Hubble time. Warp models that begin with a preformed gas disk that evolves gravitationally toward a discrete bending mode in a tilted rigid dark halo can also reproduce the observed warping of five spirals — as long as the dark halo is not too flattened, i.e., $0.6 \lesssim (c/a)_\rho \lesssim 0.9$ (Hofner & Sparke 1994). The longevity of misaligned warps in tilted halos may be limited, however; simulations with responsive halos indicate that the disk and inner halo find a common plane in a few orbital times (Dubinski & Kuijken 1995). Furthermore, Debattista & Sellwood (1999) argue that misalignment of gas and halo angular momentum can create transient warps with appropriate characteristics even in spherical halos.

The thickness of the HI gas layer in spirals is due (at least in part) to the hydrostatic balance between random gas motion and the vertical restoring force due to the total gravitational potential. By modeling the distribution and velocity of gas in the edge-on Sc NGC 4244, and taking into account systematic effects on the measured flaring due to inclination and extragalactic ionizing radiation, an axis ratio $(c/a)_\rho = 0.2_{-0.1}^{+0.3}$ is derived for the dark density in the region of the flare (Olling 1996). A portion of the uncertainty is due to the unknown anisotropy of the gas motions. A similar analysis for the Milky Way yields a considerably rounder halo $(c/a)_\rho = 0.7 \pm 0.3$ (Olling & Merrifield 1997). Applied to the edge-on NGC 891, the method gives substantially flattened density axis ratios of $0.2 < (c/a)_\rho < 0.5$ (Becquaert & Combes 1998), although non-flare models for the HI distribution and kinematics have also been put forward for this galaxy (Swaters, Sancisi & van der Hulst 1997).

Strong gravitational lensing provides a new way to measure the flattening of dark halos since the image positions and relative brightnesses are altered by the ellipticity of the foreground lensing potential. Lensing is sensitive to the total mass column along the line of sight, so modeling of luminous mass of the galaxy and any nearby dark masses (e.g., external shear) is required in order to derive accurate results, but the equilibrium assumptions required in most dynamical mass estimators play no role. Lens models often require substantially flattened density distributions with $(c/a)_\rho \lesssim 0.4$ for strong galactic lenses (Kochanek 1995, and references therein). The magnitude of the shear term required to reduce ellipticities to those representative of E and S0 galaxies may require internal shears due to misaligned dark and luminous lens mass (Keeton, Kochanek & Seljak 1997). In some cases, strict limits can be placed on the flattening of the dark lensing density, even in the presence of known external shear, as indicated in Fig. 2 which displays modeling results for a late-type lensing spiral at redshift $z=0.415$ (Koopmans, de Bruyn & Jackson 1998). Lower limits on the dark halo flattening were obtained by constraining the velocity dispersion (and thus external shear) of the neighboring galaxy with the Tully-Fisher relation and, more conservatively, with the maximum rotation velocity of massive spirals.

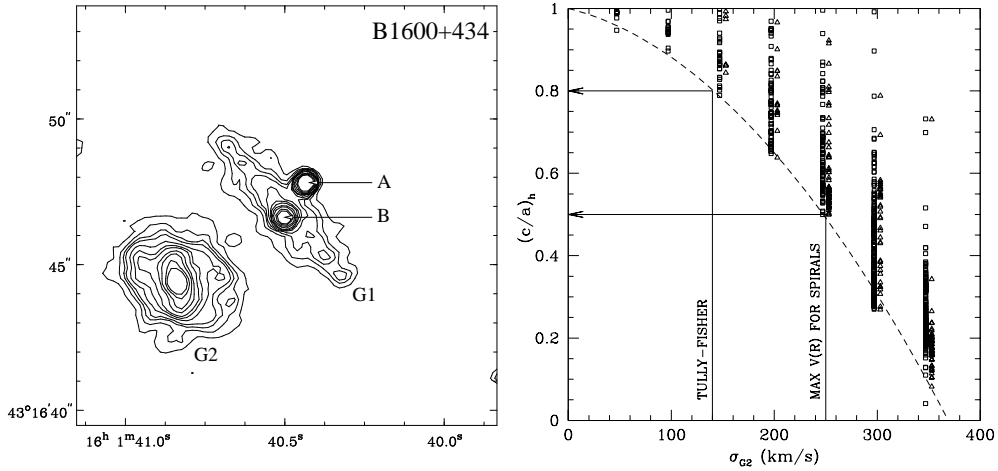


Figure 2. *Left:* Deconvolved Nordic Optical Telescope R-band image of the CLASS gravitational lens B1600+434. The edge-on lens galaxy (G1) is seen between the images A and B of the background radio source. The companion galaxy (G2) is located 4.5 arcsec southeast of G1. *Right:* The flattening $(c/a)_h$ of G1 dark halo is plotted against the velocity dispersion of the companion galaxy G2. Squares and triangles indicate a range of halo and galaxy (G1 and G2) models that fit the data. (Adapted from Koopmans, de Bruyn & Jackson 1998.)

6. Summary and Discussion

The dark halo shapes discussed here were inferred in different types of galaxies, on different spatial scales, with methods that have different systematic uncertainties and assumptions. Some systems may present special advantages that allow techniques not possible elsewhere, but may not be representative of the general population. Measurements at smaller radii may have the luxury of a wider variety of tracers and higher quality data, but are contaminated by the influence of the luminous mass. Inferred shape parameters derived at large distances safely can be assumed to probe the dark matter distribution, but may assume an equilibrium condition that is less likely to be satisfied at the large galactocentric radius of the tracer.

The contribution of the dark matter to the inner rotational support of galaxies is still not fully understood, although it appears that it is dominant in fainter, lower surface brightness galaxies. Several lines of evidence suggest that halos extend to 50 – 100 kpc; whether they extend to 200 kpc and beyond involves assessing conflicting evidence and model-dependent conclusions.

The observational evidence taken together indicates that total density distribution near the optical radius (~ 20 kpc) in spirals has an in-plane axis ratio $(b/a)_\rho \gtrsim 0.8$. If any of the measured ovalness is due to sources other than dark halo shape, dark matter halos at this radius may be even more axisymmetric. At least near the stellar body itself, dark halos are not strongly triaxial.

The inferred values for halo flattening are more disparate. Techniques that measure $(c/a)_\rho$ rather close to the equatorial plane of the stellar body return both quite spherical (precessing warps) and substantially flattened (gas layer flaring) results, even though they are applied to systems that appear to be quite similar. One might imagine that the dark potential is preferentially flattened near the equatorial plane due to the influence of the massive stellar disk; the spherical results returned by the warp analysis therefore seem to indicate that effect of the disk is negligible. Perhaps other mechanisms, like continual accretion, are responsible for shaping the distribution and velocity structure of the outer neutral hydrogen layer. It does seem clear that the gradient of the mass distribution near the galactic plane is not steep enough to suggest that the dark mass lies in a thin (<2 kpc) disk.

At heights 10 – 20 kpc above the equatorial plane, Milky Way halo star kinematics, the geometry of X-ray isophotes, and polar ring studies all indicate that the dark mass is substantially flattened with $0.3 < (c/a)_\rho < 0.7$. At these distances, there is some indication that for early-type systems the flattening of the dark and luminous mass may be similar. Polar rings with flattened halos may be more likely to capture material onto polar orbits, but this selection effect is strongly countered by the short lifetime expected for differentially precessing rings accreted at a slightly skew angle in a non-spherical potential.

How do theoretical expectations square with these observational facts? N-body simulations of dissipationless collapse produce strongly triaxial dark halos (Frenk et al. 1988, Dubinski & Carlberg 1991, Warren et al. 1992) that are both oblate and prolate and thus at strong odds with the data. Adding a small fraction ($\sim 10\%$) of dissipative gas, however, results in halos of a more consistent shape — nearly oblate, $(b/a)_\rho \gtrsim 0.8$, but moderately flattened, $(c/a)_\rho = 0.5 \pm 0.15$ (Katz & Gunn 1991, Dubinski 1994, Dubinski & Kuijken 1995). The dark halo shapes inferred from observations are thus consistent with expectations from cold dark matter simulations, as long as dissipative baryons form at least $\sim 10\%$ of the total mass within the volume relevant for the formation of the stellar galaxy.

7. A Look to the Future

What can we expect as we look toward the future? Doubtless many of the techniques discussed here will be improved, and new ones invented.

Harmonic analysis of two-dimensional velocity fields is likely to provide more detailed information about the non-axisymmetry of galactic mass distributions in different environments as the effect of spirals arms and warping is quantified. Lensing may contribute to the question of dark halo shape at many levels because, although hampered with its own difficulties, it is insensitive to the (often unknown and/or complicated) dynamical state of the system. Strong lensing, especially when applied to radio sources where extinction does not play a role in selection or altering image brightness, will become increasingly important in constraining the flattening of galactic mass distributions (see Fig. 2).

If a substantial portion of galactic dark halos is composed of compact massive objects, microlensing may help determine not only the shape but the constitution of dark halos. In the near future, the promise of using multiple lines

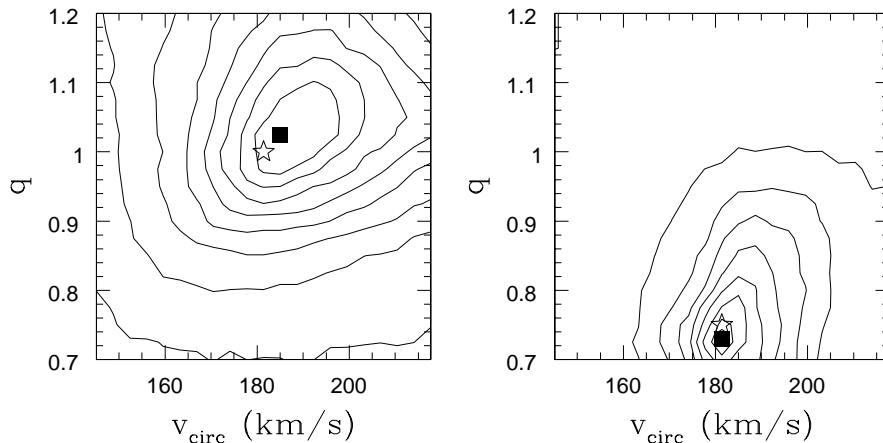


Figure 3. Contours indicate the percentage of particles (90%, 80%, 70% . . .) correctly modeled by applying an analytic description of tidal streamers in potentials of two different depths and flattenings to simulated SIM data supplemented with radial velocities. The “true” circular speed and flattening $q = (c/a)_\Phi$ of the potential is indicated with the stars; filled squares indicate the recovered halo parameters. (Adapted from Johnston et al. 1998.)

of sight (Galactic Bulge, LMC, SMC) to probe the shape of the Milky Way microlensing halo (Sackett & Gould 1993) will be hampered by small number statistics and ultimately perhaps by the possibility that a substantial number of the microlenses do not lie in the halo. If a considerable fraction of galactic dark matter *is* comprised of microlenses, projects to map the microlensing optical depth across the face of M31 will measure its intrinsic shape (Crotts 1992, Baillon et al. 1993).

Statistical weak lensing combined with redshift information is likely to become more important in constraining the outer radial profile of dark halos in a manner that is less model dependent than methods that rely on satellite dynamics. The cold kinematics and confined spatial distribution of very extended (> 50 kpc) HI features, such as tidal tails and “Leo rings” will be a welcome addition in assessing the extent of galactic halos, if they can be found in sufficient number and characterized.

Finally, the shape and extent of stellar debris trails from infalling satellites may also be an increasingly important probe of halo size and shape, especially if it can be combined with kinematical information, as may be possible with the launch of the Space Interferometry Mission (SIM) to measure proper motions of Galactic stars brighter than 20th magnitude. Simulations indicate that, if supported by ground-based programs to determine radial velocities, SIM-measured proper motions of 100 stars in a tidal stream would be sufficient to determine the circular velocity and flattening of the Galactic potential to within $\sim 2 - 3\%$ (Fig. 3) at the orbital radius of the streamer (Johnston et al. 1998.)

Acknowledgments. I am grateful to the organizing committee for travel support and to Leon Koopmans and Kathryn Johnston for preparing figures from their work for inclusion in this review.

References

- Amendt, P. & Cuddeford, P. 1994, *ApJ*, 435, 93
- Arnaboldi, M., Capaccioli, M., Cappellaro, E., Held, E..V. & Sparke, L. 1993, *A&A*, 267, 21
- Baillon, P. Bouquet, A., Giraud-Héraud, Y. & Kaplan, J. 1993, *A&A*, 277, 1
- Becquaert, J.-F. & Combes, F. 1997, *A&A*, 325, 41
- Bienaymé, O. 1999, *A&A*, 342, 86
- Binney, J, May, A. & Ostriker, J.P. 1987, *MNRAS*, 226, 149
- Brainerd, T.G., Blandford, R.D. & Smail, I. 1996, *ApJ*, 466, 623
- Bridges, T. 1999, in this volume, *Galaxy Dynamics*, eds. D. Merritt, J.A. Sellwood, J.A. & M. Valluri, Provo: ASP (astro-ph/9811136)
- Buote, D.A. & Canizares, C.R. 1996, *ApJ*, 457, 177
- Buote, D.A. & Canizares, C.R. 1997, *ApJ*, 474, 650
- Buote, D.A. & Canizares, C.R. 1998, *MNRAS*, 298, 811
- Combes, F. & Arnaboldi, M. 1996, *A&A*, 305, 763
- Courteau, S. & Rix, H.-W. 1999, *ApJ*, in press (astro-ph/9707290)
- Crotts, A.P.S. 1992, *ApJ*, 399, 43
- de Blok, W.J.G. & McGaugh, S.S. 1997, *MNRAS*, 290, 533
- Debattista, & Sellwood, J.A. 1999, *ApJ*, 513, 107L (astro-ph/9910153)
- Dubinski, J. 1994, *ApJ*, 431, 617
- Dubinski, J. & Carlberg, R. 1991, *ApJ*, 378, 496
- Dubinski, J. & Kuijken, K. 1995, *ApJ*, 442, 492
- Dubinski, J. & Mihos, J.C. & Hernquist 1996, 462, 576
- Dubinski, J. & Mihos, J.C. & Hernquist 1999, submitted to *ApJ*, (astro-ph/9902217)
- Erickson L.K., Gottesman, S.T. & Hunter, J.H. 1987, *Nature*, 325, 779
- Fasano, G., Amico, P., Bertola, F., Vio, R. & Zeilinger, W.W. 1993, *MNRAS*, 262, 109
- Franx, M. & de Zeeuw, T. 1992, *ApJ*, 392, 47L
- Franx, M. van Gorkom, J.M & de Zeeuw, T. 1994, *ApJ*, 436, 642
- Frenk, C.S., White, S.D.M, Davis, M. & Efstathiou, G. 1988, *ApJ*, 327, 507
- Hofner, P. & Sparke. L.S. 1994, *ApJ*, 428, 466
- Johnston, K.V., Zhao, H.-S., Spergel, D.N., Hernquist, L. 1998, 512L, 109
- Katz, N. & Gunn, J. E. 1991, *ApJ*, 377, 365
- Keeton, C.R., Kochanek, C.S. & Seljak, U. 1997, *ApJ*, 482, 604
- Kochanek, C.S. 1995, *ApJ*, 445, 559
- Kochanek, C.S. 1996, *ApJ*, 457, 228
- Koopmans, L.V.E, de Bruyn, A.G, & Jackson, N. 1998, *MNRAS*, 295, 534

- Kuijken, K. & Tremaine, S. 1994, *ApJ*, 421, 178
- Lambas, D.G., Maddox, S.J. & Loveday, J. 1992, *MNRAS*, 258, 404
- Lin, D.N.C., Jones, B.F. & Klemola, A.R. 1995, *ApJ*, 439, 652
- McGaugh, S.S. 1999, in this volume, *Galaxy Dynamics*, eds. D. Merritt, J.A. Sellwood, J.A. & M. Valluri, Provo: ASP (astro-ph/9812327)
- Merrifield, M.R. & Olling, R.P. 1998, *MNRAS*, 297, 943
- Mihos, J.C., Dubinski, J. & Hernquist, L. 1998, *ApJ*, 494, 183
- New, K.C.B., Tohline, J.E., Frank, J. & Vath, H.M. 1998, *ApJ*, 503, 632
- Olling, R.P. 1996, *AJ*, 112, 481
- Olling, R.P. & Merrifield, M.R. 1997, in ASP 136, *Galaxy Halos*, ed. D. Zaritsky, Provo: ASP, 219
- Pfenniger, D., Combes, F. & Martinet, L. 1994, *A&A*, 285, 79
- Palunas, P. & Williams, T.B. 1999, *AJ*, in press
- Rix, H.-W. & Zaritsky, D. 1995, *ApJ*, 447, 82
- Rix, H.-W., 1996, in IAU 169, *Unsolved Problems of the Milky Way*, eds. L. Blitz & P. Teuben, Dordrecht, Kluwer, 23 (astro-ph/9501068)
- Sackett, P.D. & Gould, A. 1993, *ApJ*, 419, 648
- Sackett, P.D., Rix, H.-W., Jarvis, B.J., Freeman, K.C. 1994, *ApJ*, 436, 629
- Sackett, P.D. & Pogge, R.W. 1995, in *Dark Matter*, eds. S.S. Holt & C.L. Bennett, New York: AIP, 141
- Sackett, P.D. 1996, in IAU 173, *Astrophysical Applications of Gravitational Lensing*, eds. C.S. Kochanek & J.N. Hewitt, Dordrecht: Kluwer, 165 (astro-ph/9508098)
- Sackett, P.D. 1997, *Pub. Astron. Soc. Australia*, 14, 11
- Schweizer, F., Whitmore, B.C. & Rubin, V.C. 1983, *AJ*, 88, 909
- Sellwood, J.A. 1999, in this volume, *Galaxy Dynamics*, eds. D. Merritt, J.A. Sellwood, J.A. & M. Valluri, Provo: ASP (astro-ph/9903184)
- Schoenmakers, R.H.M., Franx, M. & de Zeeuw, P.T. 1997, *MNRAS*, 292, 349
- Schoenmakers, R.H.M. 1998, in ASP 136, *Galaxy Halos*, ed. D. Zaritsky, 240
- Schoenmakers, R.H.M. 1999, Ph.D. Thesis, University of Groningen.
- Sommer-Larsen, J., Beers, T.C., Flynn, C., Wilhelm, R. & Christensen, P.R. 1997, *ApJ*, 481, 775
- Steiman-Cameron, T.Y., Kormendy, J. & Durisen, R.H. 1992, *AJ*, 104, 1339
- Swaters, R. 1999, in this volume, *Galaxy Dynamics*, eds. D. Merritt, J.A. Sellwood, J.A. & M. Valluri, Provo: ASP (astro-ph/9811424)
- Swaters, R.A., Sancisi, R. & van der Hulst, J.M. 1997, *ApJ*, 491, 140
- van Albada, T. & Sancisi, R. 1986, *Phil. Trans. Roy. Soc. London*, A320, 447.
- van der Marel, R.P. 1991, *MNRAS*, 248, 515
- Warren, M. S., Quinn, P. J., Salmon, J. K., & Zurek, W. H. 1992, *ApJ*, 399, 405
- Whitmore, B.C., McElroy, D., & Schweizer, F. 1987, *ApJ*, 314, 439
- Zaritsky, D. & White, S. D. M. 1994, *ApJ*, 435, 599
- Zaritsky, D. 1998, to appear in *The Galactic Halo*, (astro-ph/9810069)